REPORT DOCUMENTATION PAGE

Form Approved
OMB No. 0704-0188

PLEASE DO NOT RETURN YOUR FORM TO THE ABOVE ORGANIZATION.

1. REPORT DATE *(DD-MM-YYYY)*	2. REPORT TYPE	3. DATES COVERED *(From - To)*
01-31-2012	Final Report	From 09-30-2010 to 10-31-2011

4. TITLE AND SUBTITLE

Pulsed Plasma Arrays for Turbulence Control

5a. CONTRACT NUMBER

5b. GRANT NUMBER

FA9550-10-1-0494

5c. PROGRAM ELEMENT NUMBER

6. AUTHOR(S)

Haris J. Catrakis

5d. PROJECT NUMBER

5e. TASK NUMBER

5f. WORK UNIT NUMBER

7. PERFORMING ORGANIZATION NAME(S) AND ADDRESS(ES)

University of California, Irvine

8. PERFORMING ORGANIZATION REPORT NUMBER

9. SPONSORING/MONITORING AGENCY NAME(S) AND ADDRESS(ES)

Air Force Office of Scientific Research
Douglas Smith, Program Manager

10. SPONSOR/MONITOR'S ACRONYM(S)

AFOSR

11. SPONSOR/MONITOR'S REPORT NUMBER(S)

AFRL-OSR-VA-TR-2012-0799

12. DISTRIBUTION/AVAILABILITY STATEMENT

Distribution A

13. SUPPLEMENTARY NOTES

14. ABSTRACT

The PI successfully achieved active control of flow separation using dielectric barrier discharge plasma actuation on a hemisphere mounted on an elevated flat surface in a wind tunnel. Visualization of streaklines in the flow around the hemisphere at Re = 40,000 for control-on vs. control-off showed a reduction in the size of the separation region with active flow control. Measurement of the surface pressure coefficient also showed a recovery in the pressure coefficient for control-on vs. control-off. Velocity measurements also showed that the mean-velocity profiles and turbulence profiles were modified so that there is a minimization of the separation region. The PI explored a variational theoretical formulation which enables computation of the difference between the exact solution of the Navier-Stokes equations and a computational solution with the DOLFIN method (Dynamic Object Oriented Library for Finite Element Computation). The PI demonstrated the use of this theoretical variational formulation on its ability to generate automatically and adaptively computational grids for flow around a curved surface and active flow control. The PI computationally investigated flow separation and active flow control around a curved surface using the adaptive variationally-optimized finite element method. The PI's computational results successfully showed a significant reduction in the flow separation region by active flow control.

15. SUBJECT TERMS

16. SECURITY CLASSIFICATION OF:			17. LIMITATION OF ABSTRACT	18. NUMBER OF PAGES	19a. NAME OF RESPONSIBLE PERSON
a. REPORT	b. ABSTRACT	c. THIS PAGE		15	19b. TELEPHONE NUMBER *(Include area code)*

AFOSR Final Report

Pulsed Plasma Arrays for Turbulence Control

PI: Haris Catrakis, Program Manager: Douglas Smith

1. Experimental Aspects

This final report consists of three sections in which, respectively, the experimental, theoretical, and computational aspects of the work are described. Successful results were obtained in the 1st year of this 3-year project for a single-element plasma actuator mounted on a hemisphere. In the 2nd and 3rd years of this project, the PI would have added up to 10x10=100 plasma actuators on the hemisphere for additional results but the work was unintentionally ended prematurely in October 2011. Thus, only results of the 1st year of the project are described below. However, these results successfully show the effective use of plasma actuation on a hemisphere for substantially reducing flow separation and therefore provide a helpful basis for possible future projects on the development and demonstration of multiple plasma actuators, i.e. plasma arrays, for even more enhanced reduction of flow separation.

The three sections are also described in these 3 AIAA conference papers which the author presented in Honolulu, Hawai'i, in June 2011:

AIAA Paper 2011-3991 (Experiments), Active Control of Flow Separation on a Hemisphere with Plasma Forcing, 41st AIAA Fluid Dynamics Conference and Exhibit, 27 - 30 June 2011, Honolulu, Hawai'i

AIAA Paper 2011-4018 (Theories), Variational Theoretical Framework with Adaptive Computing of Flow Dynamics and Active Flow Control, 6th AIAA Theoretical Fluid Mechanics Conferenc, 27 - 30 June 2011, Honolulu, Hawai'i

AIAA Paper 2011-3862 (Computations), Adaptive Variationally-Optimized Computing of Flow Dynamics, Separation, and Control, 20th AIAA Computational Fluid Dynamics Conference, 27 - 30 June 2011, Honolulu, Hawaii

In the experimental work, the PI investigated active control of flow separation using dielectric barrier discharge plasma actuation on a hemisphere mounted on an elevated flat surface in a wind tunnel. Visualization of streaklines in the flow around the hemisphere at Re = 40,000 for control-on vs. control-off showed a reduction in the size of the separation region with active flow control. Measurement of the surface pressure coefficient also showed a recovery in the pressure coefficient for control-on vs. control-off. Velocity measurements also showed that the mean-velocity profiles and turbulence profiles were modified so that there is a minimization of the separation region.

Active flow control is an important field of research for many aeronautical applications [1-10] as it enables modification of flow dynamics suitable for a variety of objectives. Plasma forcing is a method of choice for active flow control in many aeronautical applications because plasma actuators have contain no moving parts [1-5, 8, 10]. In our own previous work [1], we showed that a plasma actuator can be effective in suppressing the formation of large-scale turbulent structures in a separated shear layer formed at a sharp corner.

In the experimental study for this report, we focused on active flow control of separation around a hemisphere mounted on a surface. This geometry is motivated by the use of hemispherical turrets, or other more complicated geometrical shapes, for directed-energy applications involving laser beam propagation and aero-optical effects through aircraft-generated turbulent flows. While aero-optical effects are generated by compressible flows [1], the focus of our present study is not exclusively on aero-optics. Thus, we aimed our present study on the broader challenge of flow separation from curved surfaces and as a basic practical example we therefore focus on active flow control of flow separation for incompressible flow around a hemisphere mounted on a surface.

Our experiments were conducted in an open-return wind tunnel with a test section of 1ft x 1ft cross-sectional area. The freestream speed can be adjusted up to 30m/s. The hemisphere has a radius of 7.62cm (3in) and it is mounted on an elevated platform so that a well-defined laminar boundary layer is formed instead of the boundary layer on the floor of the test section. The hemisphere is made of polypropylene material. We have machined pressure taps along the centerline of the surface of the hemisphere to enable measurement of the surface pressure coefficient profile. The flow facility is equipped with a fog machine for streakline visualizations. The Reynolds number based on the hemisphere radius and the freestream velocity of 8m/s for the current experiments is Re = 40,000. A photograph of the hemisphere without the plasma actuator is shown in figure 1. Figure 2 shows an example of our fog visualization for the flow around the hemisphere without actuator and figure 4 shows the control-on vs. control-off visualizations. In figure 2, there is clear evidence of a separated turbulent shear layer from the curved surface of the hemisphere at approximately 90 degrees elevation angle. The separated shear layer rolls up into larger-scale vortices which are shed into the wake of the hemisphere.

Our fog machine enabled our successful visualizations of streaklines around the hemisphere. We connected our fog machine to a custom machined pipe with a series of holes in order to generate a set of streaklines through the inlet of the wind tunnel. The fog fluid is water-based and consists of several glycols mixed with de-ionized water. In the fog machine, the fog fluid is moved into a heat exchanger by a pump and the heat exchanger vaporizes the fog fluid. The vaporized fog fluid rapidly expands through the nozzle of the fog machine. When the vapor mixes with cooler air outside the machine, it forms an opaque aerosol which constitutes the fog. In order to measure the pressure coefficient, we machined 22 pressure taps along the centerline of the surface of the hemisphere. These 22 pressure taps enable us to generate profiles of the pressure coefficient as a function of the elevation angle along the centerline of the hemisphere. The pressure taps were located at 1cm spacings along the centerline of the hemisphere. The pressure profile measurements provided quantitative data in addition to the flow visualizations.

Our plasma actuator consists of two copper electrodes of 3mil thickness each and a kapton dielectric of 5mil thickness which are assembled in the single dielectric barrier discharge asymmetric configuration. The plasma actuator is connected to a high voltage high frequency power supply, model PVM500, manufactured by Information Unlimited, Inc.

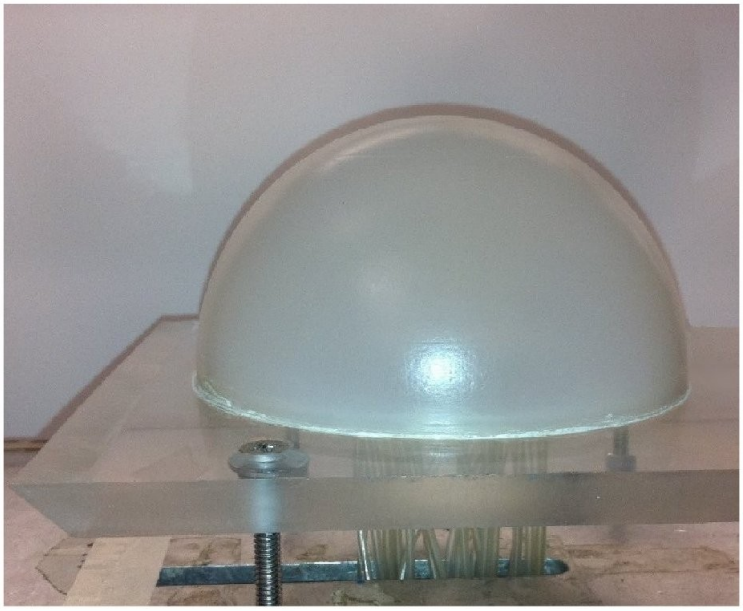

Figure 1. Photograph of our hemisphere mounted on an elevated surface in the wind tunnel without the plasma actuator.

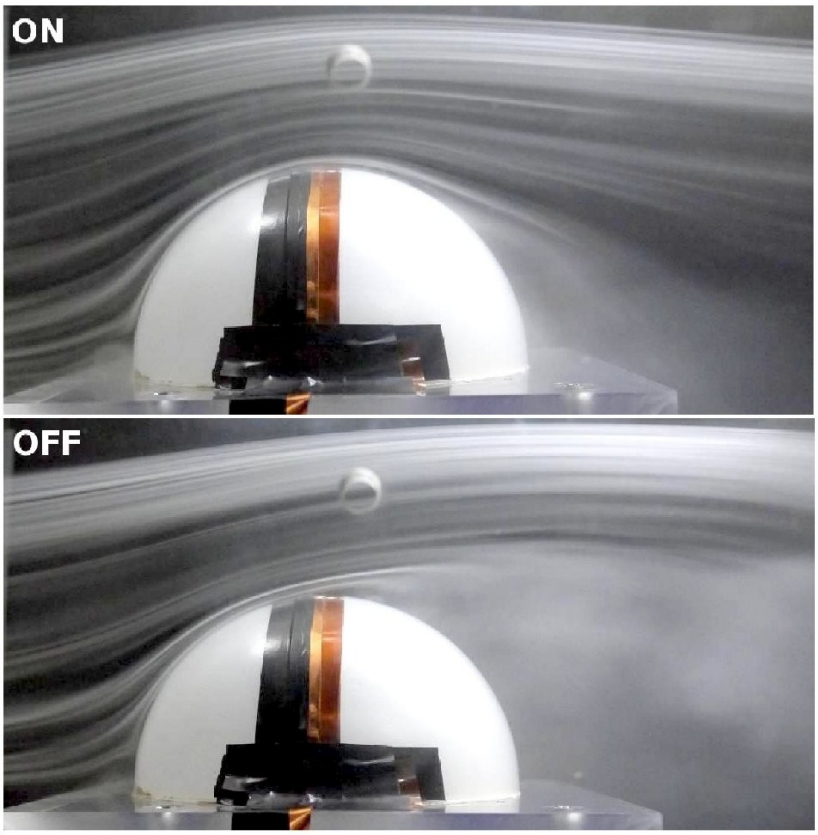

Figure 2. Photograph of our fog visualization of streaklines for the flow around the hemisphere mounted on an elevated surface in the wind tunnel without the plasma actuator.

The power supply can produce voltage up to 20kV ac peak-to-peak at a frequency from 20kHz to 50kHz and at a current of 10mA so that the power ranges up to 200W. Our settings for the current experiments are 10kV voltage, 20kHz frequency, continuously-on actuator, 10mA, and 100W. We surface mounted our plasma actuator at an elevation angle of 90 degrees on the hemisphere. A photograph of the blue light emitted by the plasma actuator on the hemisphere is shown in figure 3.

Our results for the control-off and control-on cases consist of fog visualizations of streaklines shown in figure 4 and quantitative measurements of surface pressure profiles and wake velocity profiles in figure 5. We first conducted our experiments for the baseline case, i.e. control-off, and we visualize the streaklines using a fog machine. We then turned on the plasma actuator and we conduct fog visualization for the control-on case. The flow visualizations in figure 4 show that we are able to reduce the size of the separation region and delay the flow separation angle by using plasma actuation for active flow control. The most important observation in figure 4 is that the plasma actuator is able to minimize the flow separation by moving the separation location substantially downstream along the curved surface of the hemisphere.

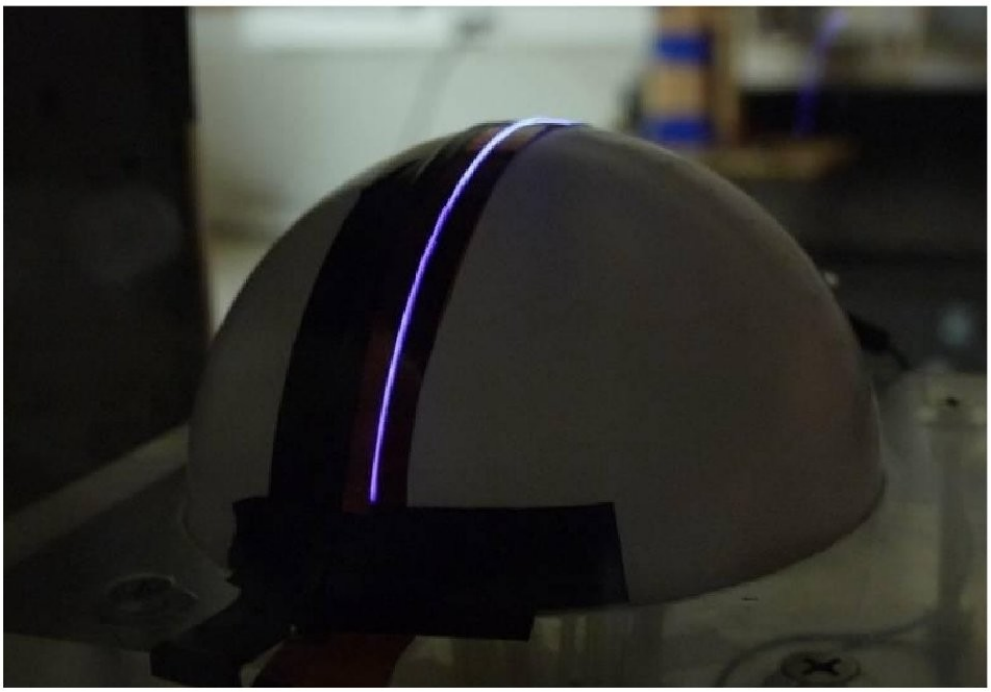

Figure 3. Photograph of the light emitted by the plasma actuator mounted on the hemisphere in the wind tunnel.

We also measured the surface pressure coefficient with the 22 surface pressure taps in order to obtain the pressure profiles for control-on vs. control-off. Figure 5 (left) shows the plots of the pressure coefficient profiles along the centerline of the hemisphere for various freestream speeds. Consistent with the fog visualizations, we see evidence of an enhanced pressure recovery on the lee side of the hemisphere when the plasma actuator is activated. This enhanced pressure recovery is consistent with the reduction in flow separation evident in our fog visualizations.

In addition, we measured the wake mean velocity profiles for control-on vs. control-off using hot-wire velocimetry. Figure 5 (right) shows the wake mean velocity profiles at a location downstream of the trailing edge of the hemisphere along the direction of the centerline axis of the hemisphere. The control-on velocity profile shows that the flow maintains its momentum to a significantly greater extent than the control-off velocity profile, consistent with reduced flow separation by the plasma actuator.

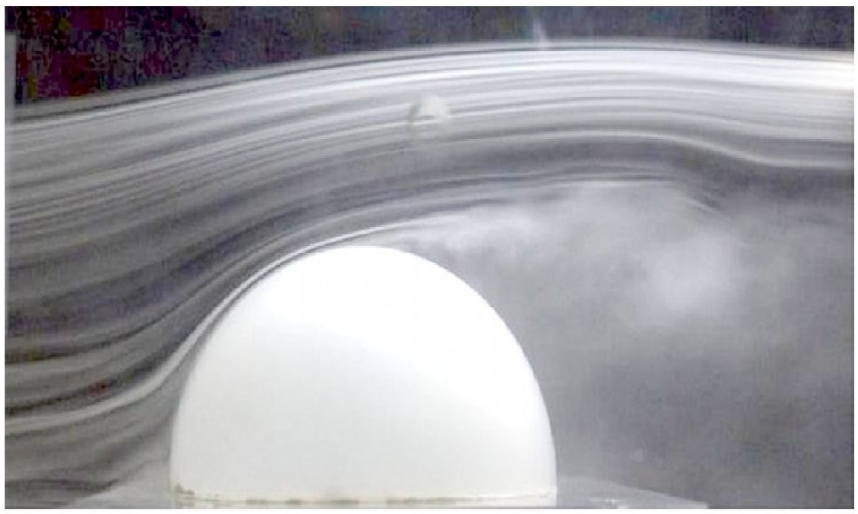

Figure 4. Photographs of fog visualizations of control-on (top) vs. control-off (bottom) flow separation on the hemisphere for freestream speed 8m/s and Reynolds number Re ~ 40,000.

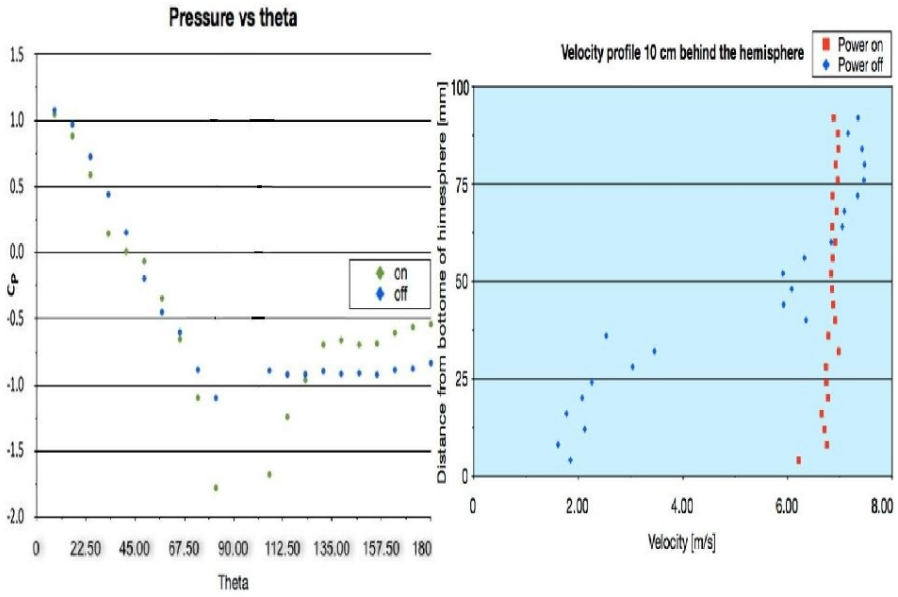

Figure 5. Surface pressure profiles (left) and wake mean velocity profiles (right) for control-on vs. control-off flow separation on the hemisphere for freestream speed 8m/s and Reynolds number Re ~ 40,000.

In summation, our experimental work focused on a wind-tunnel investigation of active control of flow separation using a dielectric barrier discharge plasma actuator on a hemisphere mounted on an elevated flat surface in a wind tunnel. Our flow conditions resulted in a Reynolds number of Re = 40,000 based on the freestream speed of 8m/s and the hemisphere radius of 7.62cm. We conducted fog visualization of streaklines in the flow around the hemisphere for control-on vs. control-off and we see a significant reduction in the size of the separation region with active flow control. We also measured the surface pressure coefficient which shows a recovery in the pressure coefficient for control-on vs. control-off. Our wake velocity measurements further confirmed our observations of successful control of the separation region. Our observations are important as comparison cases for further exploring active flow control with pulsed plasma arrays and also for conducting computations of flow control on the hemisphere.

2. Theoretical Aspects

We explored a variational theoretical formulation which enables computation of the difference between the exact solution of the Navier-Stokes equations and a computational solution with the DOLFIN method (Dynamic Object Oriented Library for Finite Element Computation) using a user-chosen global flow quantity and an auxiliary theoretical variational equation. We demonstrated the use of this theoretical variational formulation on its ability to generate automatically and adaptively computational grids for flow around a curved surface and active flow control.

Theoretical variational principles and formulations offer global methods which are useful for practical goals such as flow computations [11-17]. A helpful capability would be to have a variational formulation which can be used to compute the difference between the exact solution of the Navier-Stokes equation and a computed solution, based on a global flow quantity. Another helpful capability would be to be able to use the theoretical variational formulation and the global flow quantity in order to be able to refine computational grids with automatic adaptivity.

Such a variational formulation is possible in the framework of the DOLFIN method (Dynamic Object Oriented Library for Finite Element Computation) [13, 15-16]. In the present study, we consider a theoretical global flow quantity based on the inflow/outflow momentum and we demonstrate its utility for flow around a curved surface and for active flow control. In section II, we consider the theoretical variational formulation and we show results for flow computations. In section III, we state our conclusions and implications.

The basic theoretical idea [13, 15-16] is to consider, in addition to the variational form of the incompressible Navier-Stokes equations and the continuity equation, an auxiliary variational equation. Let us denote by u the exact solution to the Navier-Stokes equation and by u_h the numerical solution computed with the DOLFIN finite-element method. The exact solution u satisfies the forced Navier-Stokes equation and the continuity equation:

$$\frac{\partial u}{\partial t} + u \cdot \nabla u - \nu \Delta u + \nabla p = f,$$
$$\nabla \cdot u = 0.$$

The numerical solution u_h satisfies the variational finite-element form of the forced Navier-Stokes equation which is written as follows using Chorin's splitting method to perform time stepping.

$$\langle (u_h^\star - u_h^{n-1})/\Delta t_n, v\rangle + \langle \nabla u_h^{n-1} \cdot u_h^{n-1}, v\rangle + \langle \nu \nabla u_h^n, \nabla v\rangle = \langle f, v\rangle.$$

In Chorin's method, the tentative velocity is computed first by ignoring the pressure as shown above. After the tentative velocity is computed, the pressure correction is computed for evaluation of the flow velocity:

$$\begin{aligned} \langle \nabla p^n, \nabla q\rangle &= -\langle \nabla \cdot u_h^\star, q\rangle/\Delta t_n, \\ \langle u_h^n, v\rangle &= \langle u_h^\star, v\rangle - \Delta t_n \langle \nabla p^n, v\rangle. \end{aligned}$$

Conceptually, we can write the exact Navier-Stokes equation and the computational equation in terms of variational bilinear and linear forms as follows:

$$a(u, v) = L(v)$$

$$a(u_h, v) = L(v)$$

The auxiliary theoretical variational equation [13, 15-16] and its resulting use for calculating the difference between the exact solution and the computed solution, based on a global flow quantity, is as follows:

$$a^*(z, v) = \mathcal{M}(v)$$

$$\mathcal{M}(u) - \mathcal{M}(u_h) = a^*(z, u - u_h) = a(u - u_h, z) = L(z) - a(u_h, z) \equiv r(z)$$

where the a^* is the adjoint bilinear form and the script $\mathcal{M}$ is any global flow measure. The above result enables the use of this variational method for calculating the difference between the exact flow solution and the computed flow solution, based on any global flow measure, as well as for mesh refinement with automatic adaptivity.

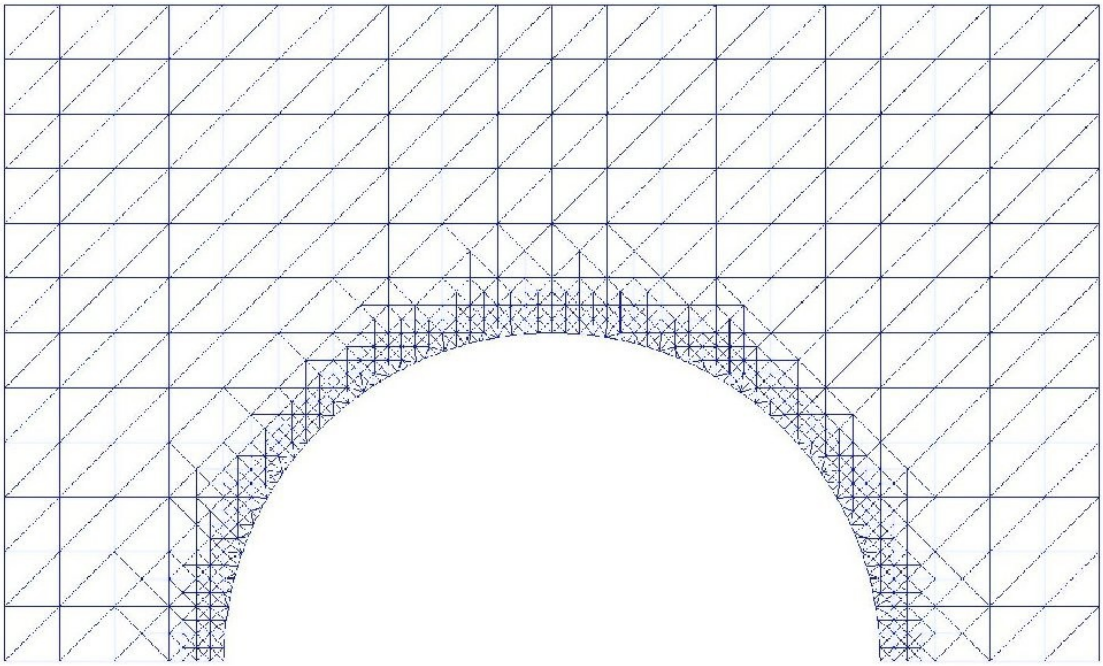

Figure 6: Initial mesh for flow around a semi-circular curved surface.

Figures 6, 7, 8, and 9 show examples of the successive refinements of a mesh for the flow around a curved surface, where we use a global flow measure consisting of the inflow/outflow momentum difference to automatically adapt the computational grid. We see that the variational formulation is able to successfully refine especially in those flow regions where it is necessary to do so such as boundary layers and separated shear layers.

Up to 14 levels of refinement were used and in each level of refinement the smallest scales were reduced by a factor of two. Starting from an initial number of 1,256 of computational elements, there are 13,329 computational elements after 14 levels of refinements. This is a much more efficient result compared to approximately (2^14)^2 = (16,384)^2 ~ 268 million computational elements otherwise. In our results, the difference between the exact solution and the computed solution after 14 levels of refinement using our global inflow/outflow momentum measure is only 2.44x10^(-14) which shows highly efficient automatic adaptivity.

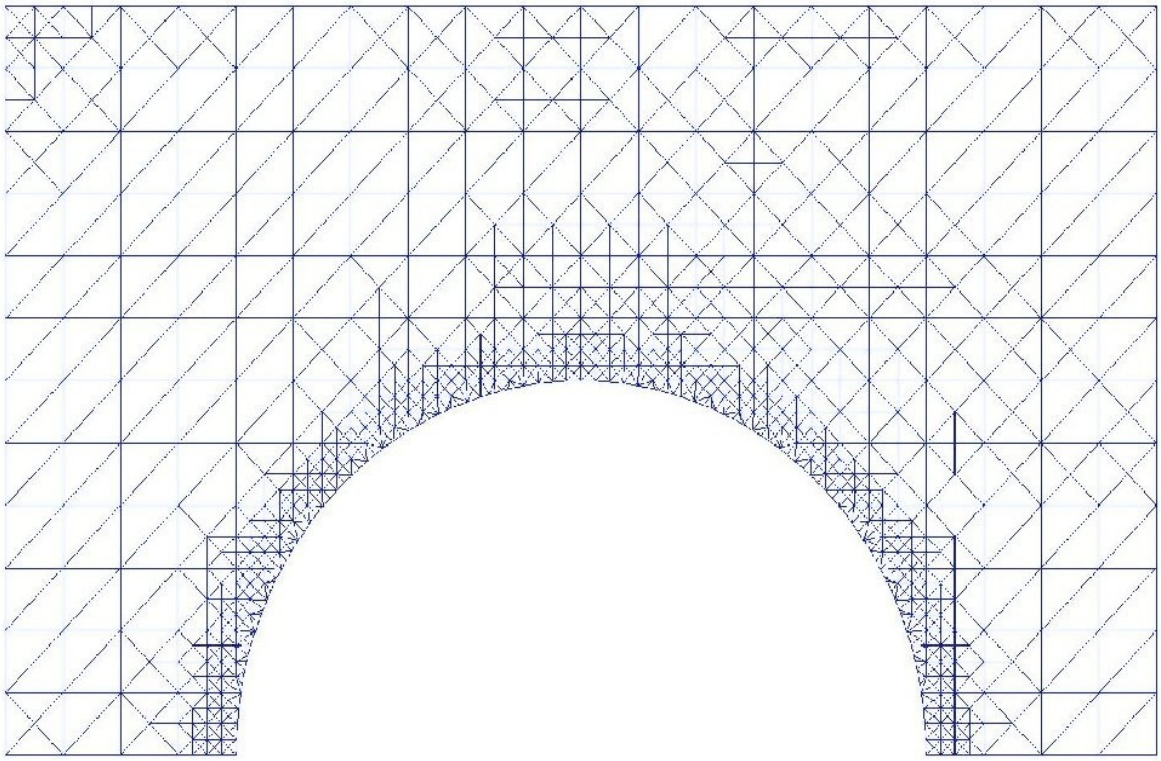

Figure 7: Automatically adapted mesh after 3 levels of refinement.

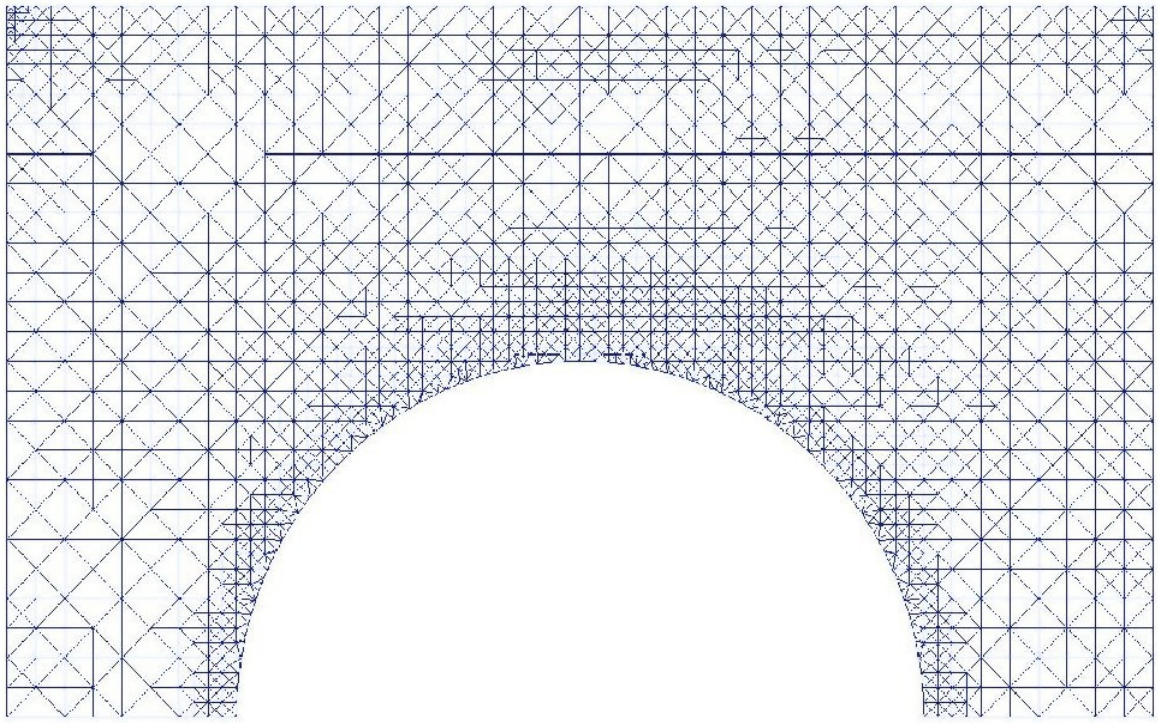

Figure 8: Automatically adapted mesh after 8 levels of refinement.

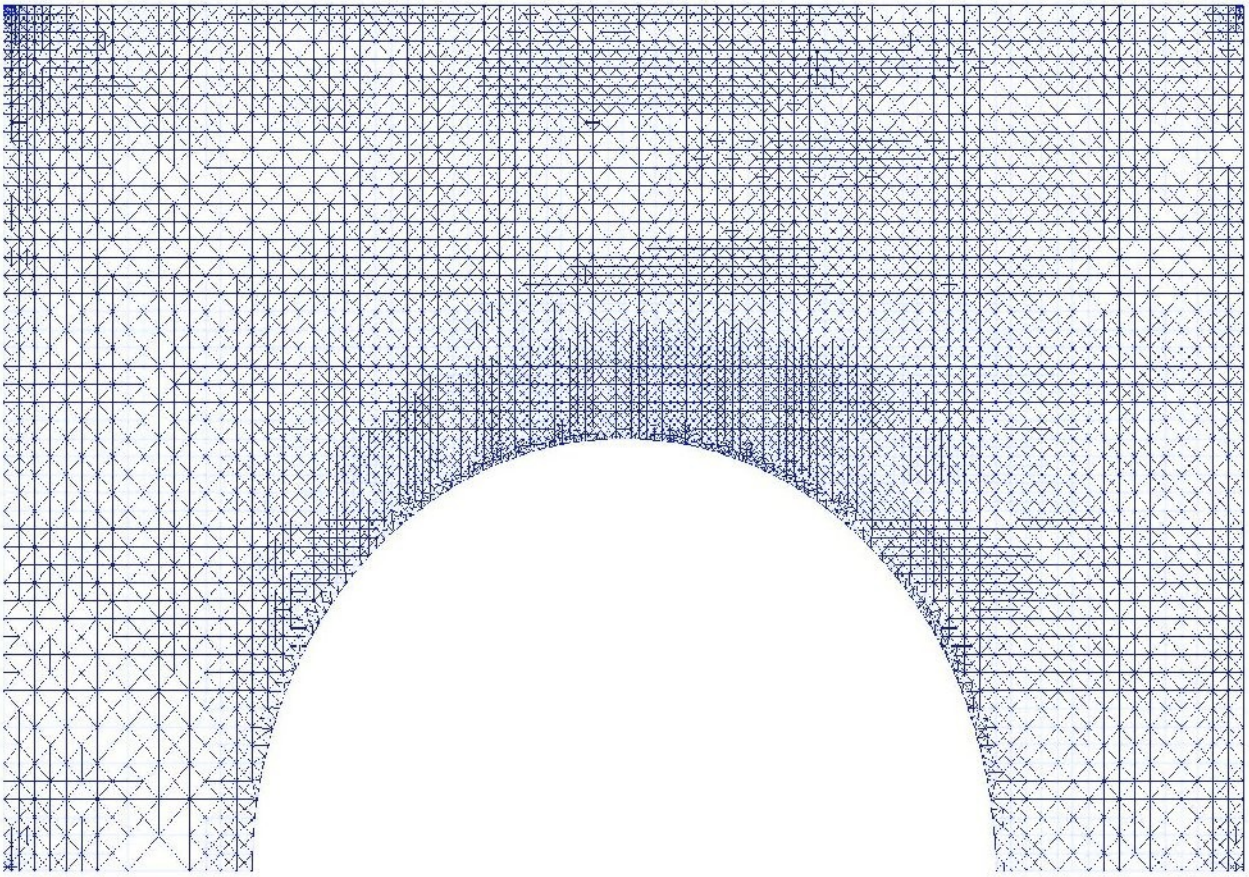

Figure 9: Automatically adapted mesh after 14 levels of refinement.

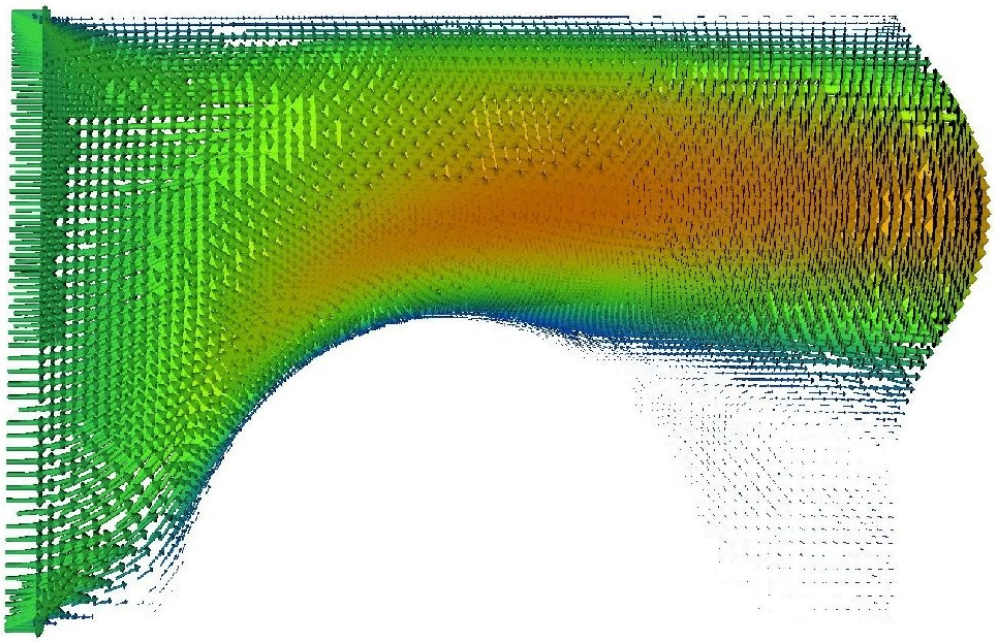

Figure 10: Flow computed around the semi-circular curved surface with the adapted mesh at 14 levels of refinement.

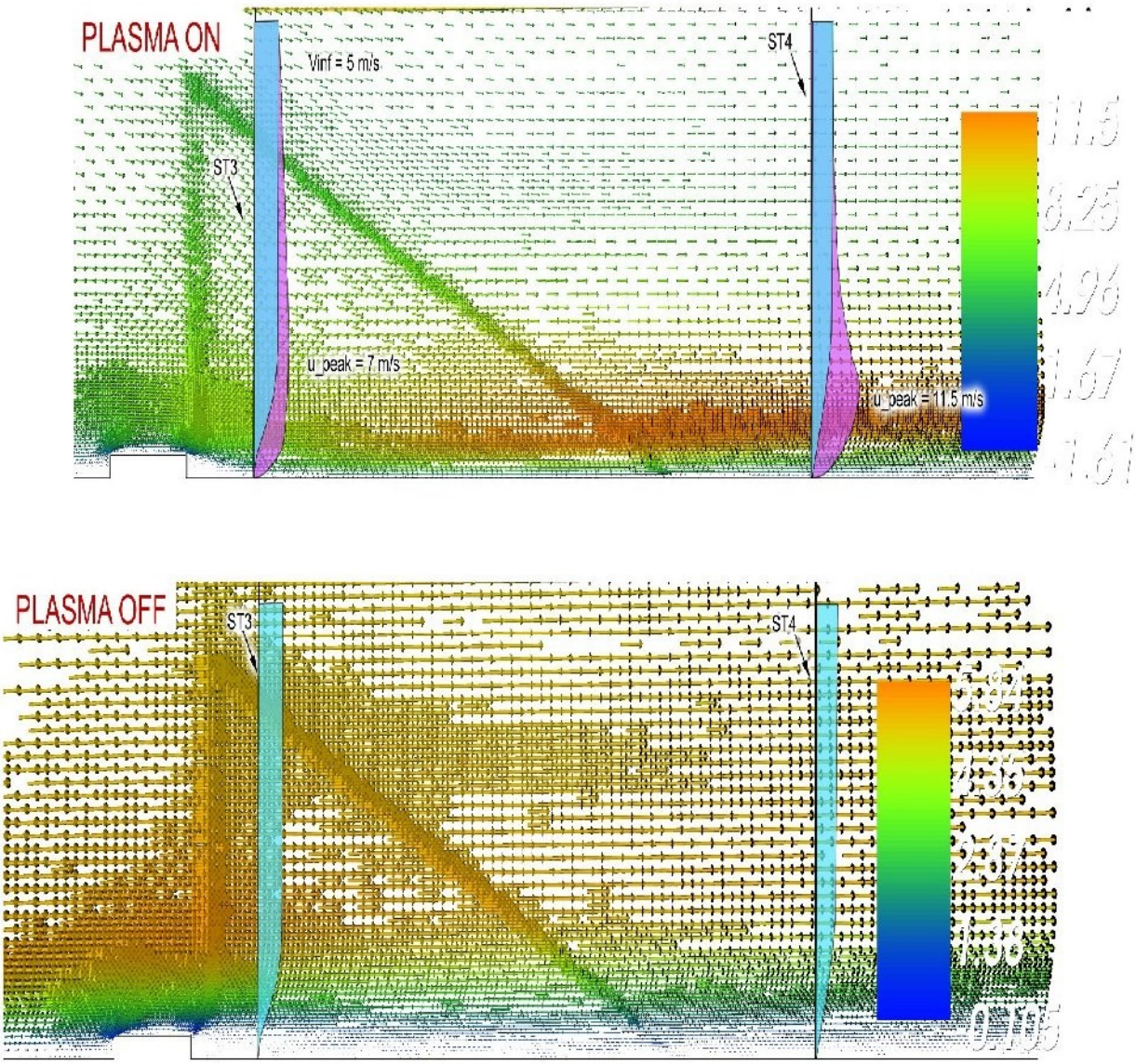

Figure 11: Active flow control results for an example of a plasma actuator on a horizontal wall.

In figure 11, we show another example of the use of the theoretical variational formulation for active flow control computations. We considered developing a first-principles plasma computational approach, but we were able to successfully use a previously-developed plasma computational model [14] which we included in our computational variational DOLFIN method to obtain consistent results for a standard horizontal-wall flow geometry [17] as shown in figure 11.

In summation, we explored the variational theoretical formulation which enables computation of the difference between the exact solution of the Navier-Stokes equations and the computational solution with the DOLFIN method (Dynamic Object Oriented Library for Finite Element Computation) using a user-chosen global flow quantity and an auxiliary theoretical variational equation. We demonstrated the use of this theoretical variational formulation on its ability to generate automatically and adaptively computational grids for flow around a curved surface and active flow control.

3. Computational Aspects

We computationally investigated flow separation and active flow control around a curved surface using an adaptive variationally-optimized finite element method. We used the DOLFIN computational method (Dynamic Object Oriented Library for Finite Element Computation) which solves the fluid dynamics equations in variational form. The variational formulation of this method enables the computational grid to be automatically adapted with a minimum number of computational elements, based on a user-chosen global flow quantity, so that there are smaller scales in those flow regions which necessitate small scales including for example flow separation regions. We obtained computational results of control-on vs. control-off for the flow around a curved surface. Our computational results showed a significant reduction in the flow separation region by active flow control.

Practical computational methods for separated flows, including the challenge of computing turbulent flow regions [11-16], need to be able to offer a balance of the advantages of DNS in some regions of the flow where all scales are resolved and LES in other regions of the flow where only the larger scales are directly resolved. For spatially three-dimensional and unsteady flow at significant Reynolds number, conducting DNS throughout the entire flow region requires a very large number of computational elements and this is very costly. In practice, therefore, a highly desirable approach will be the one which can utilize only a relatively small number of computational elements and automatically switch between DNS, in some regions of the flow, and LES, in other regions of the flow, in an adaptive manner [13]. This requires a methodology by which the grid is automatically adapted.

Such an adaptive computational method is offered by the computational set of tools known as DOLFIN (Dynamic Object Oriented Library for Finite Element Computation) as described in a number of studies [13, 15-16]. In the present study, we utilize DOLFIN to compute the flow around a curved surface mounted on a horizontal wall. This geometry is motivated by applications in which hemispherical turrets are used to direct laser energy from aircraft and, more generally, is a challenging case of flow separation over a curved three-dimensional surface and is thus relevant to all studies involving separation at unsteady locations on a curved surface.

Our computations used the DOLFIN method (Dynamic Object Oriented Library for Finite Element Computation) which enables adaptive computing with a minimum number of grid elements and therefore minimum computational cost. The DOLFIN method solves the incompressible Navier-Stokes equation in variational form. Its variational formulation includes an auxiliary variational equation which enables automatic adaptivity of the computational grid based on a user-chosen global flow quantity. We solved the incompressible Navier-Stokes equation and the continuity equation in variational discretized form with Chorin's splitting method. We used Chorin's splitting method to perform time stepping and we used different iterative solvers and different preconditioners for different steps of the solution process. In Chorin's method, one first ignores the pressure in the momentum equation and computes the tentative velocity. Then, a pressure correction is computed to evaluate the actual velocity.

At the inflow, we imposed an incoming uniform flow. This inflow developed into boundary layers at the bottom wall and top wall of the computational domain. At the outflow, we impose free flow boundary conditions. On the curved surface and on the top/bottom flat wall surfaces, we used no-slip boundary conditions. The solution was computed using continuous vector-valued piecewise quadratics

for the velocity and continuous scalar piecewise linears for the pressure (Taylor-Hood elements). To perform the adaptive mesh refinement automatically, we computed the global momentum difference between the outflow and inflow stations which DOLFIN uses in order to adaptively refine the mesh. Thus we used a minimum number of degrees of freedom optimized adaptively based on computation of the global momentum difference.

Our computations were performed in 2D at a low Reynolds number of 400 around a semicircular curve with steady flow imposed purposely in order to test this method with a future goal of extending the Reynolds number to 40,000 for 3D unsteady turbulent flows around a hemisphere and comparison with experiments we have also conducted. As stated above, our computations are adaptive in order to minimize the computational cost by using a minimum number of degrees of freedom. We start our computations with a coarse tetrahedral mesh. In subsequent iterations, the mesh is adaptively refined with respect to the inflow/outflow global momentum difference and its comparison to the exact value which is made possible by the variational formulation of this method. Figure 9 shows an example of the adaptively refined mesh after 14 mesh refinements.

The optimized adaptivity produces automatically 13,239 computational elements in figure 10 after 14 levels of refinements where in each level of refinement the smallest scales are made smaller by a factor of two. This is a significant reduction in the number of computational elements which, without automatic adaptivity, would be approximately (2^14)^2 = (16,384)^2 ~ 268 million otherwise. The difference between the adaptively computed solution and the exact solution is only 2.44x10^(-14) after 14 levels of iterations, based on the inflow/outflow global momentum difference. We emphasize again that the ability of this method to compute the difference between the numerical solution and the exact solution is made possible by its variational formulation.

Figures 11 and 12 show examples of our computational results for control-on vs. control-off for two different flow geometries. Figure 12 shows our successful computational results of active flow control on a semi-circular curved wall where the plasma actuator is located at an elevation angle of 90 degrees. The flow Reynolds number and plasma actuator settings are the same as for our hemisphere experiments. In other words, in figure 12 the plasma actuator is located at an elevation angle of 90 degrees on a semi-circular curved surface for otherwise similar flow conditions as in figure 10 which represents the baseline control-off case. We see in figure 12 that our computations successfully reduce the extent of the flow separation region for the control-on case, also shown with our experiments, in comparison to the control-off case. Our successful flow control results were achieved as part of our effort to eventually compute active flow control for 3D higher Reynolds number unsteady turbulent flows such as the flow around a hemisphere.

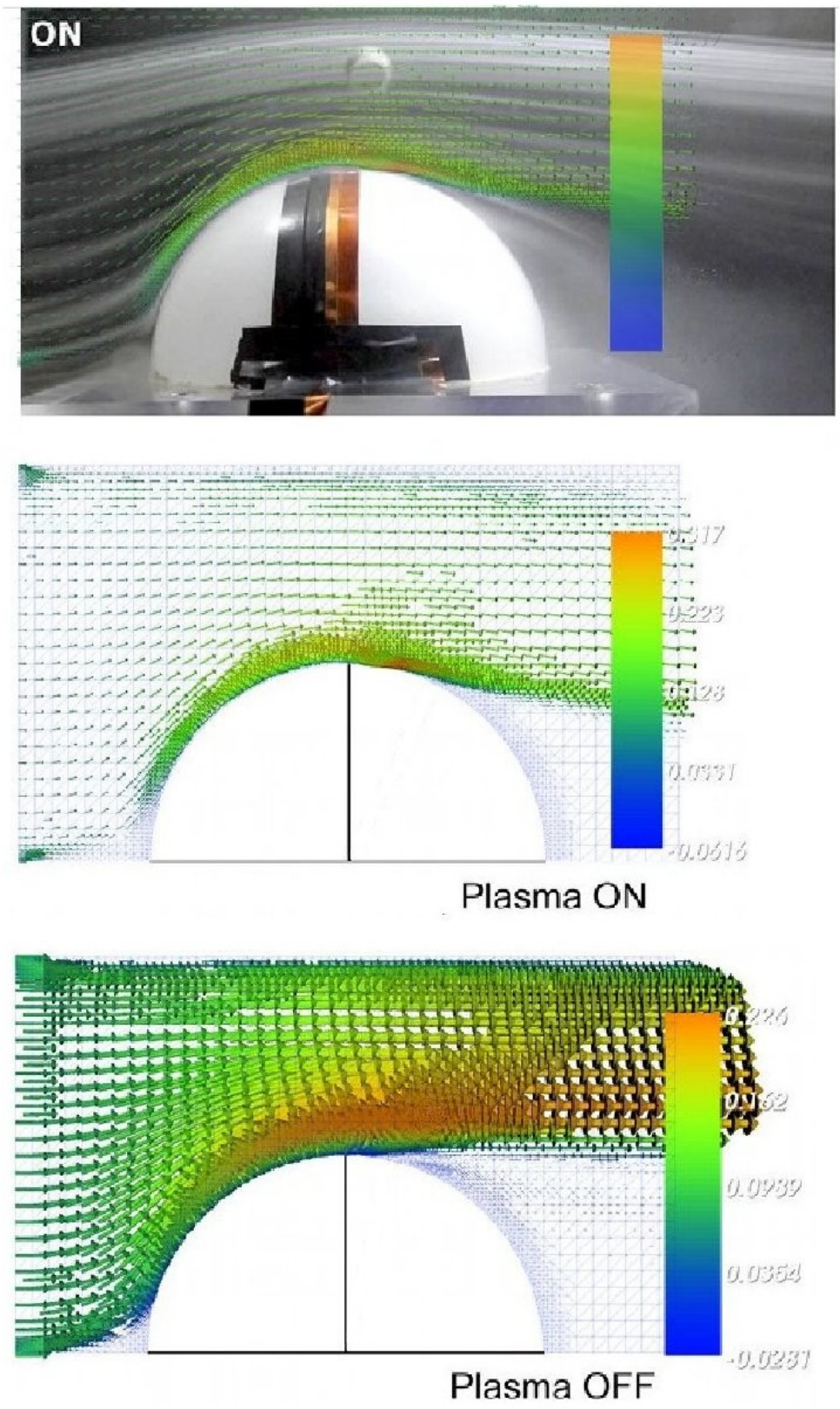

Figure 12: Examples of our computational results of active flow control-on (top/middle) vs. control-off (bottom) on the semi-circular curved surface with comparison (top) to our hemisphere experiments.

In summation, our computational investigations of flow separation and active flow control around a curved surface were conducted using DOLFIN (Dynamic Object Oriented Library for Finite Element Computation) and a plasma computational model. The DOLFIN computational method has a variational formulation which enabled automatic adaptivity of the computational mesh. This generated a minimum number of computational elements with minimum computational cost. The adaptivity produced smaller scales in regions which necessitated small scales such as flow separation regions. This adaptivity was achieved based on a user-chosen global flow quantity and the variational formulation of this method. Our results showed successful computations of active flow control with plasma actuation on a curved surface.

References

[1] Freeman, A. P. & Catrakis, H. J., Direct Reduction of Aero-Optical Aberrations by Large Structure Suppression Control in Turbulence, *AIAA J.*, Vol. 46, No. 10, pp. 2582-2590, 2008.
[2] Corke, T. C., Enloe, C. L., & Wilkinson, S. P., Dielectric Barrier Discharge Actuators for Flow Control, *Annu. Rev. Fluid Mech.*, Vol. 42, pp. 505-529, 2010.
[3] Enloe, C. L., McLaughlin, T. E., VanDyken, R. D., Kachner, K. D., Jumper, E. J., Corke, T. C., Post, M., & Haddad, O., Mechanisms and Responses of a Single-Dielectric Barrier Plasma Actuator: Geometric Effects, *AIAA J.*, Vol. 42, pp. 595-604, 2004.
[4] Corke, T. C., Post, M. L. & Orlov, D. M., SDBD Plasma Enhanced Aerodynamics: Physics, Modeling, and Applications, *Exp. Fluids*, Vol. 46, pp. 1-26, 2009.
[5] Cattafesta, L. N. & Sheplak, M., Actuators for Active Flow Control, *Ann. Rev. Fluid Mech.*, Vol. 43, pp. 247-272, 2011.
[6] Vukasinovic, B., Brzozowski, D., and Glezer, A., Fluidic Control of Separation Over a Hemispherical Turret, *AIAA J.*, Vol. 47, pp. 2212-2222, 2009.
[7] Vukasinovic, B., Glezer, A., Gordeyev, S., Jumper, E., and Kibens, V., Active Control and Optical Diagnostics of the Flow over a Hemispherical Turret, AIAA Paper 2008-598, 2008.
[8] He, C., Corke, T. C., & Patel, M. P., Numerical and Experimental Analysis of Plasma Flow Control Over a Hump Model, AIAA Paper 2007-0935, 45th AIAA, Reno, Jan. 8-11, 2007.
[9] Choi, H., Jeon, W.-P., & Kim, J., Control of Flow Over a Bluff Body, *Ann. Rev. Fluid Mech.*, Vol. 40, pp. 113-139, 2008.
[10] Corke, T. C., Post, M. L. & Orlov, D. M., SDBD Plasma Enhanced Aerodynamics: Concepts, Optimization & Applications, *Prog. Aero. Sci.*, Vol. 43, pp. 193-217, Oct-Nov 2007.
[11] Peterson, M. & Rubinstein, Y., Turbulence on a Desktop, Computing in Science and Engineering, Vol. 3, No. 3, pp. 86-94, May/June, 2001.
[12] Lesieur, M., Metais, O., & Comte, P., Large-Eddy Simulations of Turbulence, Cambridge U. Press, New York, 2005.
[13] Hoffman, J. & Johnson, C., "A New Approach to Computational Turbulence Modeling", Chalmers Finite Element Center, Chalmers University of Technology, Goteborg, Sweden, Preprint 2004-08, 2004.
[14] Rizzetta, D. P. & Visbal, M. R., Numerical Investigations of Plasma-Based Control for Low-Reynolds Number Airfoil Flows, AIAA 2010-4255, pp. 1-22, 2010.
[15] Hoffman, J., "Computation of Mean Drag for Bluff Body Problems Using Adaptive DNS/LES", *SIAM J. Sci. Comput.*, Vol. 27, No. 1, pp. 184-207, 2005.
[16] Hoffman, J. & Johnson, C., "Computational Turbulent Incompressible Flow", Springer Verlag, 2007.
[17] Shyy, W., Jayraman, B., & Andersson, A., Modeling of Glow Discharge-Induced Fluid Dynamics, J. Appl. Phys., Vol. 92, No. 11, pp. 6434-6443, 2002.